



ELSEVIER

Available online at [www.sciencedirect.com](http://www.sciencedirect.com)

SCIENCE @ DIRECT®

International Journal of Non-Linear Mechanics 39 (2004) 1079–1091

INTERNATIONAL JOURNAL OF

**NON-LINEAR  
MECHANICS**

[www.elsevier.com/locate/nlm](http://www.elsevier.com/locate/nlm)

# Non-linear dynamics of a system of coupled oscillators with essential stiffness non-linearities

Alexander F. Vakakis<sup>a,b</sup>, Richard H. Rand<sup>c,\*</sup>

<sup>a</sup>*Division of Mechanics, School of Applied Mathematical and Physical Sciences, National Technical University of Athens, P.O. Box 64042, GR-157 10 Zografos, Greece*

<sup>b</sup>*Department of Mechanical and Industrial Engineering, University of Illinois, 1206 W. Green Street, Urbana, IL 61801, USA*

<sup>c</sup>*Department of Theoretical and Applied Mechanics, Cornell University, Ithaca, NY 14853, USA*

Received 8 November 2002; received in revised form 21 April 2003; accepted 2 June 2003

## Abstract

We study the resonant dynamics of a two-degree-of-freedom system composed of a linear oscillator weakly coupled to a strongly non-linear one, with an essential (non-linearizable) cubic stiffness non-linearity. For the undamped system this leads to a series of internal resonances, depending on the level of (conserved) total energy of oscillation. We study in detail the 1:1 internal resonance, and show that the undamped system possesses stable and unstable synchronous periodic motions (non-linear normal modes—NNMs), as well as, asynchronous periodic motions (elliptic orbits—EOs). Furthermore, we show that when damping is introduced certain NNMs produce resonance capture phenomena, where a trajectory of the damped dynamics gets ‘captured’ in the neighborhood of a damped NNM before ‘escaping’ and becoming an oscillation with exponentially decaying amplitude. In turn, these resonance captures may lead to passive non-linear energy pumping phenomena from the linear to the non-linear oscillator. Thus, sustained resonance capture appears to provide a dynamical mechanism for passively transferring energy from one part of the system to another, in a one-way, irreversible fashion. Numerical integrations confirm the analytical predictions.

© 2003 Elsevier Ltd. All rights reserved.

*Keywords:* Non-linear; Resonance; Capture; Coupled oscillators

## 1. Introduction

We consider the dynamics of a two degree-of-freedom (DOF) system of weakly coupled oscillators with cubic stiffness non-linearities. In the limit of zero

coupling the system decomposes into two single-DOF subsystems: A linear oscillator with normalized natural frequency equal to unity, and a non-linear oscillator possessing a non-linearizable cubic stiffness. We are interested in studying the dynamics of the weakly coupled system.

Previous works (for example [1,2]) analyzed the dynamics of systems with internal, external and combination resonances, by partitioning the dynamics into ‘slow’ and ‘fast’ components and reducing the analysis to a small set of modulation equations governing

\* Corresponding author. Tel.: +1-607-255-7145; fax: +1-607-255-2011.

*E-mail addresses:* [vakakis@central.ntua.gr](mailto:vakakis@central.ntua.gr),  
[avakakis@uiuc.edu](mailto:avakakis@uiuc.edu) (A.F. Vakakis), [rhr2@cornell.edu](mailto:rhr2@cornell.edu)  
(R.H. Rand).

the slow-flow, i.e., the evolution of the ‘slow’ dynamics of the system. Generally, internal resonances introduce interesting bifurcations to the free and forced dynamics, and lead to essentially non-linear dynamical phenomena that have no counterparts in linear theory. In recent works, a comprehensive classification of the possible internal resonances in discrete non-linear oscillators was performed by [3,4].

In this work we focus on the 1:1 internal resonance between the linear and non-linear oscillators and apply asymptotic techniques to study the free dynamics when no damping exists. Depending on the system parameters, stable and unstable synchronous periodic solutions (non-linear normal modes—NNMs) or asynchronous periodic motions are detected, along with homoclinic loops in the ‘slow’ flow dynamics. Numerical simulations confirm the analytical predictions. When damping is introduced, certain of these homoclinic loops can be transformed to domains of attraction for resonance capture [5,6]. In turn, resonance capture leads to passive energy pumping [7,8] from the linear to the non-linear oscillator. Following [6] we provide a direct link between resonance capture and passive non-linear energy pumping in the damped system of coupled oscillators. We utilize analytical and numerical techniques to analyze these interesting dynamical phenomena.

**2. Statement of the problem**

We are interested in the dynamics of a system of two oscillators, one of which is strictly non-linear with cubic non-linearity. The oscillators are assumed to be coupled by small non-linear (cubic) terms. If we neglect damping, the problem is defined by the following equations:

$$\frac{d^2x}{dt^2} + x = -\varepsilon \frac{\partial V}{\partial x}, \tag{1}$$

$$\frac{d^2y}{dt^2} + y^3 = -\varepsilon \frac{\partial V}{\partial y}, \tag{2}$$

where  $\varepsilon \ll 1$  and where  $V$  is given by

$$V = a_{40}x^4 + a_{31}x^3y + a_{22}x^2y^2 + a_{31}xy^3. \tag{3}$$

We study this system by first using the method of averaging to obtain a slow flow valid to  $O(\varepsilon)$ , and then analyzing the slow flow.

**3. Averaging**

In order to perturb off of the  $\varepsilon = 0$  system, we need to solve the equation:

$$\frac{d^2y}{dt^2} + y^3 = 0. \tag{4}$$

The exact solution to Eq. (4) is

$$y(t) = A \operatorname{cn}(At; k) \quad \text{where } k = 1/\sqrt{2} \tag{5}$$

and  $A$  is an arbitrary constant.

As shown in [9–12], variation of parameters for the equation

$$\frac{d^2y}{dt^2} + y^3 = \varepsilon f \tag{6}$$

takes the form

$$\frac{dA}{dt} = \varepsilon f \frac{cn'}{A}, \tag{7}$$

$$\frac{d\phi}{dt} = \frac{A}{4K} - \varepsilon f \frac{cn}{4KA^2}, \tag{8}$$

where  $cn' = \partial \operatorname{cn}(u, k) / \partial u$ , where  $u = 4K\phi$ , and where  $\phi = At/4K$ .

Here the solution of Eq. (6) has been taken in the form

$$y = A \operatorname{cn}(4K\phi, k) \tag{9}$$

where the modulus  $k = 1/\sqrt{2}$  and the elliptic integral of the first kind  $K(k) = 1.854$ .

We simplify the averaging by use of an ‘‘engineering’’ approximation. Byrd and Friedman [13, p. 304], give the following Fourier expansion for  $cn$ :

$$cn \frac{2K}{\pi} q = 0.955 \cos q + 0.043 \cos 3q + \dots \tag{10}$$

where here  $K = K(1/\sqrt{2}) = 1.854$ .

We replace Eq. (10) by the following approximation (after Chirikov [14]):

$$cn \frac{2K}{\pi} q \approx \cos q. \tag{11}$$

Using Eq. (11), Eq. (9) becomes

$$y = A \cos \theta \quad \text{where } \theta = 2\pi\phi. \tag{12}$$

Using this approximation (12) for  $y$ , the variation of parameter Eqs. (7), (8) become

$$\frac{dA}{dt} = -\varepsilon f \frac{\pi}{2KA} \sin \theta, \tag{13}$$

$$\frac{d\theta}{dt} = \frac{\pi A}{2K} - \varepsilon f \frac{\pi}{2KA^2} \cos \theta. \tag{14}$$

The corresponding treatment of the  $x$ -equation follows the usual lines (see [15, Chapter 3], for example). For the equation:

$$\frac{d^2x}{dt^2} + x = \varepsilon g, \tag{15}$$

we take  $x$  in the form

$$x = R \cos \psi, \tag{16}$$

whereupon variation of parameters gives:

$$\frac{dR}{dt} = -\varepsilon g \sin \psi, \tag{17}$$

$$\frac{d\psi}{dt} = 1 - \varepsilon g \frac{\cos \psi}{R}. \tag{18}$$

Now if we let  $f = -\partial V/\partial y$  in Eq. (6), and  $g = -\partial V/\partial x$  in Eq. (17), then Eqs. (13), (14), (17), (18) represent the result of variation of parameters for the original system (1), (2), where  $y$  and  $x$  are related to the state variables  $A, \theta$  and  $R, \psi$ , respectively, through Eqs. (12), (16).

The next step is to replace  $x$  and  $y$  in Eqs. (13), (14), (17), (18) by their equivalents in  $A, \theta$  and  $R, \psi$  via Eqs. (12), (16). Using computer algebra, we obtain the following equation for  $dR/dt$ , and three similar equations on  $dA/at$ ,  $d\psi/dt$  and  $d\theta/dt$ , which we omit

listing for brevity:

$$\begin{aligned} \frac{dR}{dt} = & \frac{a_{13} A^3 \varepsilon \sin(3\theta + \psi)}{8} - \frac{a_{13} A^3 \varepsilon \sin(3\theta - \psi)}{8} \\ & + \frac{a_{22} A^2 \varepsilon R \sin(2\theta + 2\psi)}{4} \\ & - \frac{a_{22} A^2 \varepsilon R \sin(2\theta - 2\psi)}{4} \\ & + \frac{3a_{31} A \varepsilon R^2 \sin(\theta + 3\psi)}{8} \\ & + \frac{3a_{31} A \varepsilon R^2 \sin(\theta + \psi)}{8} + \frac{3a_{13} A^3 \varepsilon \sin(\theta + \psi)}{8} \\ & - \frac{3a_{31} A \varepsilon R^2 \sin(\theta - \psi)}{8} - \frac{3a_{13} A^3 \varepsilon \sin(\theta - \psi)}{8} \\ & - \frac{3a_{31} A \varepsilon R^2 \sin(\theta - 3\psi)}{8} + \frac{a_{40} \varepsilon \sin(4\psi) R^3}{2} \\ & + a_{40} \varepsilon \sin(2\psi) R^3 + \frac{a_{22} A^2 \varepsilon \sin(2\psi) R}{2}. \end{aligned} \tag{19}$$

Next, we apply the method of averaging to these “variation of parameters” equations. We posit a near-identity transformation (see [15]) for each of the variables  $R, A, \psi, \theta$ . For example for  $R$  this takes the form

$$R = \bar{R} + \varepsilon w_1(\bar{R}, \bar{A}, \bar{\psi}, \bar{\theta}), \tag{20}$$

where  $w_1$  is a generating function which will be chosen so as to simplify the resulting slow flow as much as possible. Differentiating Eq. (20),

$$\begin{aligned} \frac{dR}{dt} = & \frac{d\bar{R}}{dt} + \varepsilon \left( \frac{\partial w_1}{\partial \bar{R}} \frac{d\bar{R}}{dt} + \frac{\partial w_1}{\partial \bar{A}} \frac{d\bar{A}}{dt} \right. \\ & \left. + \frac{\partial w_1}{\partial \bar{\psi}} \frac{d\bar{\psi}}{dt} + \frac{\partial w_1}{\partial \bar{\theta}} \frac{d\bar{\theta}}{dt} \right). \end{aligned} \tag{21}$$

By inspection of Eqs. (13), (14), (17), (18), we see that Eq. (21) becomes, neglecting terms of  $O(\varepsilon^2)$ ,

$$\begin{aligned} \frac{dR}{dt} = & \frac{d\bar{R}}{dt} + \varepsilon \left( \frac{\partial w_1}{\partial \bar{\psi}} + \frac{\partial w_1}{\partial \bar{\theta}} \frac{\bar{A}}{\mu} \right) \\ & \text{where } \mu = 2K/\pi = 1.18. \end{aligned} \tag{22}$$

Now we substitute Eq. (22) into the  $dR/dt$  Eq. (19) and choose  $w_1$  to eliminate as many terms as possible

from the RHS of the d.e. As an example, take the following term:

$$\begin{aligned} \frac{dR}{dt} &= \frac{d\bar{R}}{dt} + \varepsilon \left( \frac{\partial w_1}{\partial \bar{\psi}} + \frac{\partial w_1}{\partial \bar{\theta}} \frac{\bar{A}}{\mu} \right) \\ &= -\frac{3\varepsilon \bar{A} \bar{R}^2 a_{31}}{8} \sin(\bar{\theta} - \bar{\psi}). \end{aligned} \tag{23}$$

We choose  $w_1 = C \cos(\bar{\theta} - \bar{\psi})$  and substitute, allowing us to solve for  $C$ :

$$C = \frac{(3\varepsilon \bar{A} \bar{R}^2 a_{31}/8)}{(\bar{A}/\mu) - 1}. \tag{24}$$

Proceeding in this way, we eliminate all terms from the RHS of Eq. (19) and from the RHSs of the comparable equations on  $dA/at$ ,  $d\psi/dt$  and  $d\theta/dt$ , except for those terms which have no trig multiplier. These terms would require that  $w_1$  include terms proportional to  $t$ , which would fail to permit expansion (20) to be uniformly valid for large  $t$ . We obtain the following non-resonant slow flow (where we have dropped the bars for convenience):

$$\frac{dA}{dt} = 0, \tag{25}$$

$$\frac{dR}{dt} = 0, \tag{26}$$

$$\frac{d\psi}{dt} = 1 + \frac{\varepsilon a_{22}}{2} A^2 + \frac{3\varepsilon a_{40}}{2} R^2, \tag{27}$$

$$\frac{d\theta}{dt} = \frac{A}{\mu} + \frac{\varepsilon a_{22}}{2\mu} \frac{R^2}{A}. \tag{28}$$

Eqs. (27), (28) give expressions for the frequency-amplitude relations of the non-linear normal modes which correspond respectively to the uncoupled  $x$ - and  $y$ -motions in the non-resonant case.

**4. Investigation of the 1:1 resonance**

Note that the denominator of the derived coefficient  $C$  in Eq. (24) vanishes when  $A = \mu$ . (Recall that  $\mu = 2K/\pi = 1.18$ , see Eq. (22).) This means that the term  $-\frac{3\varepsilon \bar{A} \bar{R}^2 a_{31}}{8} \sin(\bar{\theta} - \bar{\psi})$  in Eq. (23) is resonant. The vanishing of the argument of the trig term is responsible for the resonance. Inspection of the

variation of parameter equations shows that there are three resonant conditions:  $\theta = \psi$ ,  $\theta = 3\psi$ ,  $3\theta = \psi$ . These correspond respectively to the following amplitudes  $A$  of the strictly non-linear  $y$ -oscillator:  $A = \mu = 1.18$ ,  $A = 3\mu = 3.54$ ,  $A = \mu/3 = 0.393$ .

In order to investigate what happens close to the 1:1 resonance, that is, when  $A \approx \mu = 1.18$ , we omit removing the terms which cause the resonance. Writing  $v = \theta - \psi$ , we obtain

$$\begin{aligned} \frac{dR}{dt} &= \\ &= -\frac{A\varepsilon(2Aa_{22}R \sin 2v + 3a_{31}R^2 \sin v + 3A^2a_{13} \sin v)}{8} \end{aligned} \tag{29}$$

$$\begin{aligned} \frac{dA}{dt} &= \\ &= \frac{\varepsilon R(2Aa_{22}R \sin 2v + 3a_{31}R^2 \sin v + 3A^2a_{13} \sin v)}{8A\mu} \end{aligned} \tag{30}$$

$$\begin{aligned} \frac{dv}{dt} &= \frac{A}{\mu} - 1 - \frac{3a_{40}\varepsilon R^2}{2} + \frac{a_{22}\varepsilon R^2}{2A\mu} - \frac{A^2 a_{22}\varepsilon}{2} \\ &+ \frac{a_{22}\varepsilon R^2 \cos 2v}{4A\mu} - \frac{A^2 a_{22}\varepsilon \cos 2v}{4} \\ &+ \frac{3a_{31}\varepsilon R^3 \cos v}{8A^2\mu} - \frac{9Aa_{31}\varepsilon R \cos v}{8} \\ &+ \frac{9a_{13}\varepsilon R \cos v}{8\mu} - \frac{3A^3 a_{13}\varepsilon \cos v}{8R}. \end{aligned} \tag{31}$$

This three-dimensional system can be simplified by dividing Eq. (29) by Eq. (30), giving

$$\frac{dR}{dA} = -\mu \frac{A^2}{R}. \tag{32}$$

Integrating Eq. (33), we obtain the first integral:

$$\frac{R^2}{2} + \mu \frac{A^3}{3} = k_1 = \text{constant}. \tag{33}$$

A second first integral is

$$\begin{aligned} \frac{R^2}{2} + \frac{A^4}{4} + \varepsilon \left[ \frac{3}{8} a_{40}R^4 + \frac{1}{8} a_{22}A^2R^2 (2 + \cos 2v) \right. \\ \left. + \frac{3}{8} (a_{13}A^2 + a_{31}R^2)AR \cos v \right] \\ = k_2 = \text{constant}. \end{aligned} \tag{34}$$

This last result may be checked by differentiating (34) with respect to  $t$  and substituting the slow flow Eqs. (29)–(31).

These first integrals may be viewed as surfaces in the  $R - A - v$  slow flow phase space which has topology  $R^+ \times R^+ \times S^1$ . In particular, for a given value of  $k_1$ , which is found from the initial conditions  $R(0)$  and  $A(0)$ , Eq. (33) is a cylindrical surface parallel to the  $v$ -axis. We shall be interested in the nature of the slow flow on this surface. For a given value of  $k_2$ , the surface (34) intersects the cylinder (33) in a curve. By allowing  $k_2$  to vary, the cylinder (33) becomes foliated into invariant curves.

### 5. Slow flow equilibria

Equilibria of the slow flow Eqs. (29)–(31) correspond to periodic motions in the original Eqs. (1), (2). In order to obtain expressions for these slow flow equilibria and to investigate their stability, we proceed as follows: We solve Eq. (33) for  $R$  and substitute the resulting expression in Eqs. (30) and (31) to obtain two equations in  $A$  and  $v$  of the form

$$\frac{dA}{dt} = F(A, v), \quad \frac{dv}{dt} = G(A, v). \tag{35}$$

The equilibrium condition in the first of these equations,  $F(A, v) = 0$ , can be satisfied in three ways:

$$v = 0 \text{ or } v = \pi \text{ or}$$

$$\cos v = -\frac{3(a_{31}R(A)^2 + A^2a_{13})}{4Aa_{22}R(A)}, \tag{36}$$

where  $R(A)$  represents the function of  $A$  obtained by solving Eq. (33) for  $R$ :

$$R(A) = \sqrt{\frac{2}{3}} \sqrt{3k_1 - \mu A^3}. \tag{37}$$

Note that since we are interested in 1:1 resonance,  $A \approx \mu = 2K/\pi = 1.18$  and Eq. (37) tells us that  $k_1 > \mu A^3/3 \approx \mu^4/3 = 0.646$ .

Thus the number of slow flow equilibria in the case of 1:1 resonance is either 2 or 4, depending upon whether or not the third condition in (36) has real roots. The bifurcation case corresponds to  $\cos v = \pm 1$ . Substituting  $A = \mu$  into this limiting case, we obtain

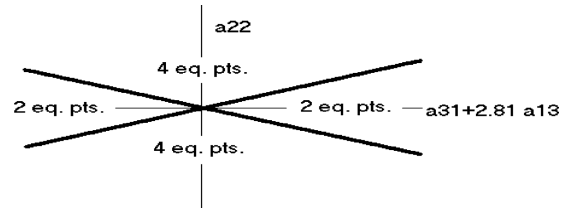


Fig. 1. Bifurcation diagram.

the following relation between the parameters:

$$a_{22} = \frac{\pm\sqrt{3} (2(3k_1 - \mu^4)a_{31} + 3\mu^2a_{13})}{4\sqrt{2}\mu\sqrt{3k_1 - \mu^4}}. \tag{38}$$

As an example, we choose the value of  $k_1$  to correspond to the initial conditions  $R(0) = A(0) = 1$  which gives  $k_1 = 0.893333$ , in which case Eq. (38) becomes

$$a_{22} = \pm 0.4468(a_{31} + 2.8178a_{13}), \tag{39}$$

giving the following bifurcation diagram (Fig. 1).

Next, we investigate the stability of these slow flow equilibria. Let us select one of the conditions (36) and call it  $v = v^*$ . Using this condition in the equilibrium condition for the second of (35),  $G(A, v) = 0$ , we obtain

$$G(A, v^*) = 0. \tag{40}$$

We seek to satisfy this equation approximately by choosing  $A$  in the form

$$A = \mu + \epsilon u + O(\epsilon^2). \tag{41}$$

Let us denote by  $u^*$  and  $A^* = \mu + \epsilon u^*$  the resulting equilibrium location. The nature of the equilibrium may be obtained by linearizing in its neighborhood:

$$\frac{d(A - A^*)}{dt} = (A - A^*) \frac{\partial F}{\partial A} + (v - v^*) \frac{\partial F}{\partial v} + \dots \tag{42}$$

$$\frac{d(v - v^*)}{dt} = (A - A^*) \frac{\partial G}{\partial A} + (v - v^*) \frac{\partial G}{\partial v} + \dots \tag{43}$$

where the partial derivatives are evaluated at the equilibrium  $(A^*, v^*)$ . From the existence of the second first integral (and the absence of dissipation in the original equations of motion) we know that the trace of the Jacobian matrix of Eqs. (42), (43) must vanish. Thus the type of equilibrium is determined by the

determinant  $\Delta$  of the Jacobian matrix:

$$\Delta > 0 \Rightarrow \text{center}, \quad \Delta < 0 \Rightarrow \text{saddle.} \quad (44)$$

We now give the result of computations. We begin with  $u^*$ :

$$u^* = a_{31} \left( -\frac{11 \cos v^* \mu^6}{12\sqrt{2}q} + \frac{13k_1 \cos v^* \mu^2}{4\sqrt{2}q} - \frac{3k_1^2 \cos v^*}{2\sqrt{2}\mu^2 q} \right) + a_{13} \left( \frac{9 \cos v^* \mu^4}{8\sqrt{2}q} - \frac{9k_1 \cos v^*}{4\sqrt{2}q} \right) + a_{40}(3k_1\mu - \mu^5) + a_{22} \left( \frac{5 \cos 2v^* \mu^3}{12} + \frac{5\mu^3}{6} - \frac{k_1 \cos 2v^*}{2\mu} - \frac{k_1}{\mu} \right), \quad (45)$$

where  $q = \sqrt{k_1 - (\mu^4/3)}$  and where  $\mu = 2K/\pi = 1.18$ . As an example, we again choose  $k_1 = 0.893333$ , in which case Eq. (45) becomes

$$u^* = 1.00759a_{31} \cos v^* + 0.24343a_{13} \cos v^* + 0.87464a_{40} + (0.61213 + 0.30607 \cos 2v^*)a_{22}. \quad (46)$$

For these parameters, the determinant  $\Delta$  of the Jacobian matrix is computed to be

$$\Delta = -0.17744\varepsilon[a_{22} \cos 2v^* + 0.4468 \cos v^*(a_{31} + 2.8178a_{13})]. \quad (47)$$

Thus from (44) we may conclude that the type of equilibrium occurring at  $v = v^*$  is dependent on the sign of the following quantity:

$$a_{22} \cos 2v^* + 0.4468 \cos v^*(a_{31} + 2.8178a_{13}) < 0 \Rightarrow \text{center} > 0 \Rightarrow \text{saddle.} \quad (48)$$

Now we apply these results to the slow flow equilibria at  $v^* = 0$  and  $v^* = \pi$ :

$$a_{22} \pm 0.4468(a_{31} + 2.8178a_{13}) < 0 \Rightarrow \text{center} > 0 \Rightarrow \text{saddle,} \quad (49)$$

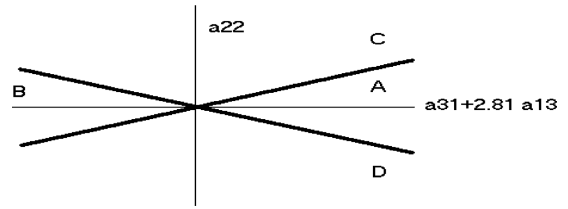


Fig. 2. Four cases.

where the upper sign refers to  $v^* = 0$  and the lower sign refers to  $v^* = \pi$ . By comparing conditions (49) to conditions (39), which govern whether or not there are two equilibria in addition to  $v^* = 0$  and  $\pi$ , we may draw the following conclusions:

If  $v^* = 0$  and  $\pi$  are the only two equilibria, then they have opposite types. If the quantity  $a_{31} + 2.8178a_{13} > 0$  then  $v^* = 0$  is a saddle and  $v^* = \pi$  is a center. If the quantity  $a_{31} + 2.8178a_{13} < 0$  then  $v^* = 0$  is a center and  $v^* = \pi$  is a saddle.

If there are two additional equilibria coming from the third condition of Eq. (36), then  $v^* = 0$  and  $\pi$  both are of the same type, and the additional equilibria are of the opposite type. If  $a_{22} > 0$  then  $v^* = 0$  and  $v^* = \pi$  are saddles while the additional equilibria are centers. If  $a_{22} < 0$  then  $v^* = 0$  and  $v^* = \pi$  are centers while the additional equilibria are saddles.

These considerations lead to a graphical enumeration of the four cases shown in Figs. 2 and 3.

These results may be checked by computing Poincare maps directly from the original o.d.e.'s (1)–(3) for the corresponding parameters. The choice of the constant  $k_1 = 0.89333$  in Fig. 3 will correspond to a corresponding value of the energy  $h$ , where

$$h = \frac{1}{2}(\dot{x}^2 + \dot{y}^2) + \frac{1}{2}(x^2 + y^2) + \varepsilon V. \quad (50)$$

Using Eqs. (12), (16) and neglecting terms of  $O(\varepsilon)$ , this becomes

$$h = \frac{1}{2}R^2 + \frac{1}{4}A^2. \quad (51)$$

In the case of 1:1 resonance, we had the approximate first integral (33):

$$\frac{R^2}{2} + \mu \frac{A^3}{3} = k_1 = \text{constant.} \quad (52)$$

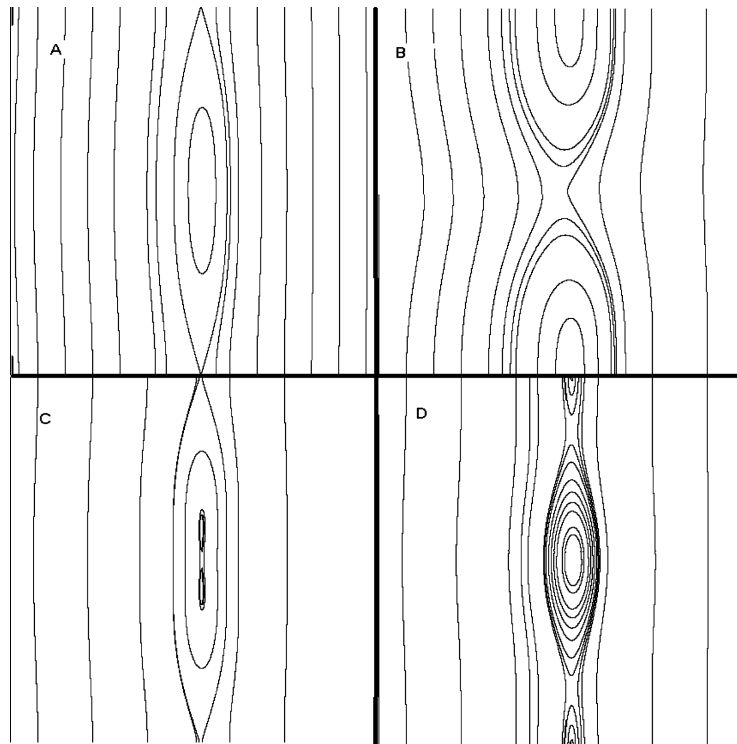


Fig. 3. Phase portraits of the four cases. In each case the slow flow on the cylinder (33) is shown projected onto the  $R-v$  plane. The horizontal axis goes from  $R = 0$  to 1.336, and the vertical axis goes from  $v = 0$  to  $2\pi$ . The parameters for the four cases are as follows: A ( $a_{31} = 1, a_{13} = 1, a_{22} = 1, a_{40} = 1$ ), B ( $a_{31} = -4, a_{13} = -4, a_{22} = 6, a_{40} = 1$ ), C ( $a_{31} = 1, a_{13} = 1, a_{22} = 2, a_{40} = 1$ ), D ( $a_{31} = 1, a_{13} = 1, a_{22} = -3, a_{40} = 1$ ). In each case  $k_1 = 0.89333$ .

Subtracting (52) from (51) we obtain

$$h - k_1 = \frac{1}{4}A^4 - \mu \frac{A^3}{3}. \tag{53}$$

But for 1:1 resonance we saw in Eq. (41) that  $A = \mu + O(\varepsilon)$ , giving

$$h = k_1 - \frac{1}{12}\mu^2 = 0.7318, \tag{54}$$

where we have used  $k_1 = 0.89333$  and  $\mu = 1.18$ .

Figs. 4 and 5 present the results of such computations cases C,D, respectively. In each case the surface of section for the Poincare map is taken as  $x = 0$  with  $\dot{x} > 0$ . Initial conditions were chosen to generate the motions corresponding to the separatrices in Fig. 3. The excellent qualitative agreement between Figs. 4, 5 and 3 demonstrates the validity of our asymptotic expansions.

The fixed points in the Poincare maps correspond to periodic motions in the original system (1)–(3). We note that Figs. 4, 5 illustrate two different types of periodic motions. The fixed points which occur on the vertical ( $\dot{y}$ ) axis correspond to motions in which  $y = 0$  occurs simultaneously with  $x = 0$ . These periodic motions are called non-linear normal modes (NNMs) and may be thought of as vibrations-in-unison, or synchronous periodic motions. If projected onto the  $x-y$  plane, NNMs plot as curves which pass through the origin.

In addition, Figs. 4 and 5 also possess fixed points which occur off the vertical axis. Such motions are also periodic, but they do not pass through the origin when projected onto the  $x-y$  plane. Rather they plot as closed curves on the  $x-y$  plane, approximately elliptical in shape, and are known as elliptic orbits (EOs). These motions are not vibrations-in-unison, and are said to be asynchronous.

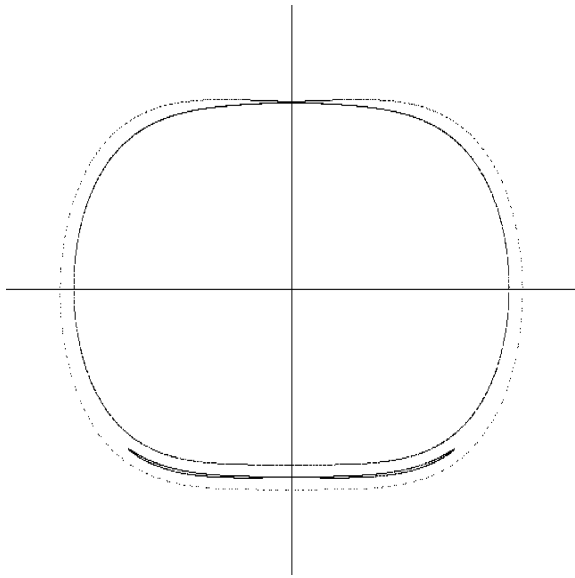


Fig. 4. Poincaré map, case C. The  $y-\dot{y}$  plane is displayed, extending from  $-1.5$  to  $+1.5$  along both axes. Eqs. (1)–(3) were numerically integrated using initial conditions which lie on the energy surface  $h = 0.7318$ . See text.

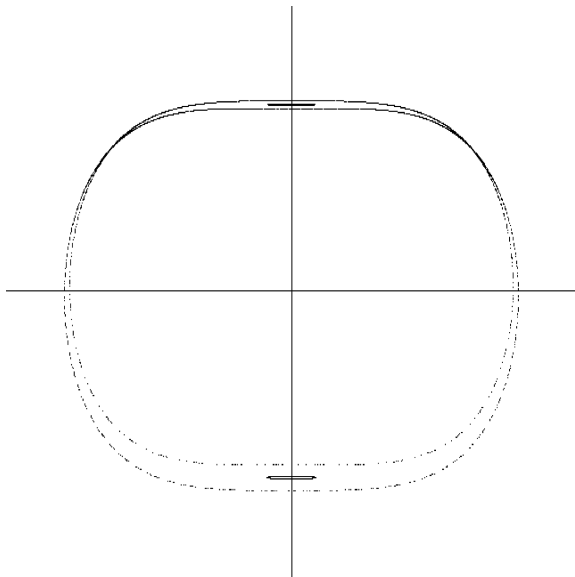


Fig. 5. Poincaré map, case D. The  $y-\dot{y}$  plane is displayed, extending from  $-1.5$  to  $+1.5$  along both axes. Eqs. (1)–(3) were numerically integrated using initial conditions which lie on the energy surface  $h = 0.7318$ . See text.

### 6. Example

Consider a system of two unit masses which are constrained to move along a straight line, and which are restrained by three springs, two of which are anchor springs and one of which is a coupling spring. One anchor spring is linear with spring constant  $k_1$ ,  $F = k_1\delta$ . The other two springs are strictly cubic,  $F = k_i\delta^3$ ,  $i = 2, 3$ . See Fig. 6.

The potential energy may be written:

$$P.E. = \frac{1}{2} k_1 x^2 + \frac{1}{4} k_2 (x - y)^4 + \frac{1}{4} k_3 y^4. \quad (55)$$

We rewrite this by collecting terms, in the following form:

$$P.E. = \frac{1}{2} k_1 x^2 + \frac{1}{4} k_2 \times (x^4 - 4x^3 y + 6x^2 y^2 - 4x y^3) + \frac{1}{4} (k_3 + k_2) y^4. \quad (56)$$

We take  $k_1 = 1$ ,  $k_2 = \varepsilon$ , and  $k_3 = 1 - \varepsilon$ , giving

$$P.E. = \frac{1}{2} x^2 + \frac{1}{4} \varepsilon \times (x^4 - 4x^3 y + 6x^2 y^2 - 4x y^3) + \frac{1}{4} y^4 \quad (57)$$

which gives the equations of motion:

$$\ddot{x} + x = -\varepsilon V_x, \quad \ddot{y} + y^3 = -\varepsilon V_y \quad \text{where}$$

$$V = \frac{1}{4} (x^4 - 4x^3 y + 6x^2 y^2 - 4x y^3). \quad (58)$$

This is a special case of the general potential  $V$

$$V = a_{40} x^4 + a_{31} x^3 y + a_{22} x^2 y^2 + a_{13} x y^3 \quad (59)$$

in which

$$a_{40} = 1, \quad a_{31} = -4, \quad a_{22} = 6, \quad a_{13} = -4. \quad (60)$$

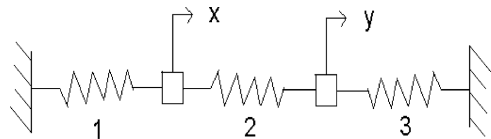


Fig. 6. Example system consisting of two unit masses and three springs. Spring 1 is linear, while springs 2 and 3 are non-linear. See text.

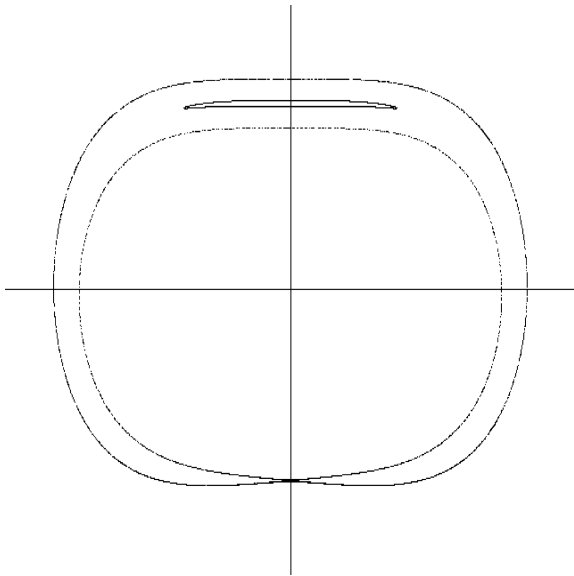


Fig. 7. Poincaré map, case B. The  $y-\dot{y}$  plane is displayed, extending from  $-1.5$  to  $+1.5$  along both axes. Eqs. (1)–(3) were numerically integrated using initial conditions which lie on the energy surface  $h = 0.7318$ . See text.

This case has been called case B in Fig. 3. The corresponding Poincaré map is shown in Fig. 7 for  $\varepsilon=0.001$  and  $h = 0.7318$ . Cut is  $x = 0, \dot{x} > 0$ , and  $y-\dot{y}$  plane is displayed from  $-1.5$  to  $1.5$  in both directions.

**7. Resonance capture and passive non-linear energy pumping in the damped system**

To study the effect of damping on the dynamics we focus on the specific example of two coupled oscillators just considered (case B). By adding two viscous damping terms the equations of motion take the form:

$$\ddot{x} + x + \varepsilon\lambda\dot{x} + \varepsilon(x - y)^3 = 0, \tag{61}$$

$$\ddot{y} + (1 - \varepsilon)y^3 + \varepsilon\lambda\dot{y} + \varepsilon(y - x)^3 = 0. \tag{62}$$

In Fig. 8 we depict the damped response of the system with parameters  $\varepsilon = 0.1, \lambda = 0.5$  and zero initial conditions except for  $\dot{x}(0) = 1.6$ . These initial conditions correspond to an impulse of magnitude 1.6 applied to the linear oscillator, with the system initially at rest.

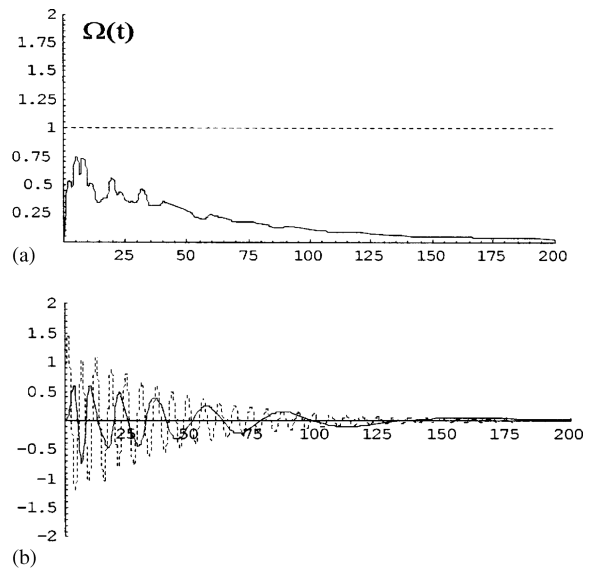


Fig. 8. Case of no resonance capture: (a) Instantaneous frequency of the non-linear oscillator, (b) Response of the linear (dashed line) and non-linear (solid line) oscillator.

In Fig. 8a we present the approximate instantaneous frequency of the non-linear oscillator computed by [7]

$$\Omega = \Xi I_1^{1/3}(t), \tag{63}$$

where

$$\Xi = \left( \frac{3\pi^4(1 - \varepsilon)}{8K^4} \right)^{1/3},$$

$$I_1(t) = \left( \frac{\pi^2 \dot{y}^2}{2A^2 \Xi^2 K^2} + \frac{y^4(t)}{A^4} \right)^{3/4}, \tag{64}$$

in which

$$A = \left( \frac{1}{4(1 - \varepsilon)} \right)^{1/6} \left( \frac{3\pi}{K} \right)^{1/3}, \tag{65}$$

and  $K = K(1/2)$  is the complete elliptic integral of the first kind with modulus  $1/2$ . From Fig. 8a we note that due to the relatively low level of initial excitation,  $\Omega(t)$  does not reach the neighborhood of the natural frequency of the linear oscillator, and, as a result no resonance capture and no significant energy pumping from the linear to the non-linear oscillator takes place. This is concluded from Fig. 8b where the time responses of the two oscillators are depicted.

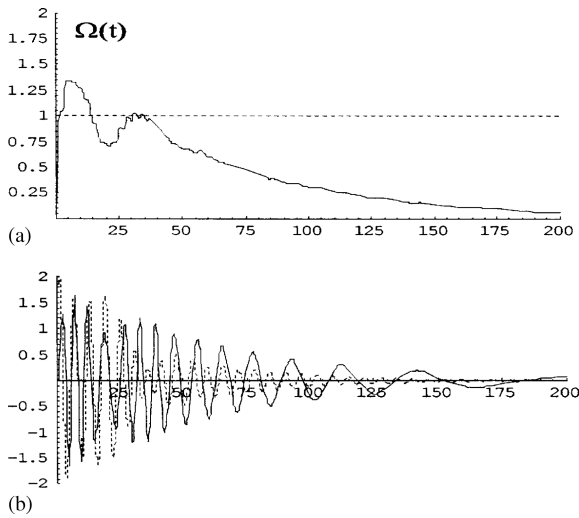


Fig. 9. Case of resonance capture: (a) Instantaneous frequency of the non-linear oscillator, (b) Response of the linear (dashed line) and non-linear (solid line) oscillator.

In Fig. 9 we show the response of the same system, but for the higher initial velocity  $\dot{x}(0) = 3.0$ . For this increased level of initial excitation we see that the instantaneous frequency of the non-linear oscillator reaches the neighborhood of the natural frequency of the linear oscillator, giving rise to 1:1 resonance capture. It can be concluded from Fig. 9b that significant energy transfer from the linear to the non-linear oscillator takes place. As discussed below, this energy transfer (pumping) can be directly related to the resonance capture phenomenon.

For comparison purposes in Fig. 10 we depict the portion of total energy dissipated at the viscous damper of the non-linear oscillator versus time for each of the two cases discussed above. For low initial energy (no energy pumping) nearly 9% of total energy is dissipated, whereas, when energy pumping occurs, as much as 45% of total energy is dissipated. This clearly demonstrates the capacity of the non-linear oscillator to absorb energy from the linear one as the level of initial excitation increases.

In order to better understand the dynamics of the 1:1 resonance capture and its relation to energy pumping we will perform an analysis based on the partition of the damped response into ‘slow’ and ‘fast’ parts. This partition is justified by the numerical

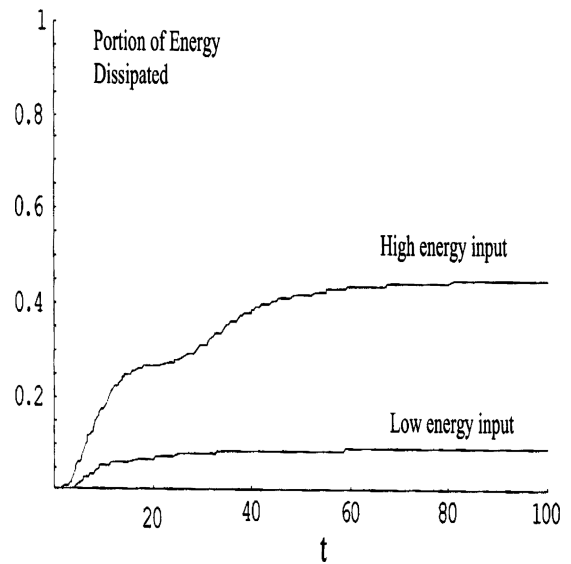


Fig. 10. Portion of initial energy dissipated at the damper of the non-linear oscillator versus time.

simulations of Figs. 8b and 9b where it is observed that fast oscillations are modulated by slowly varying envelopes. Moreover, from Fig. 9b we see that 1:1 resonance capture takes place when the fast oscillation has frequency approximately equal to unity (the frequency of the linear oscillator). It is concluded that in the energy capture regime the fast oscillations have frequency approximately equal to unity. We follow the analytical technique first introduced by Manevitch [16], by introducing the complex variables,

$$\psi_1 = \dot{y} + jy, \psi_2 = \dot{x} + jx, \quad j = \sqrt{-1} \quad (66)$$

and complexifying the resulting equations of motion (61), (62):

$$\begin{aligned} \dot{\psi}_1 - \left( \frac{j - \varepsilon\lambda}{2} \right) (\psi_1 + \psi_1^*) + \frac{j}{8} (1 - \varepsilon)(\psi_1 - \psi_1^*)^3 \\ + \frac{j\varepsilon}{8} (\psi_1 - \psi_2 - \psi_1^* + \psi_2^*)^3 = 0, \end{aligned} \quad (67)$$

$$\begin{aligned} \dot{\psi}_2 - j\psi_2 + \frac{\varepsilon\lambda}{2} (\psi_2 + \psi_2^*) + \frac{j}{2} (\psi_2 - \psi_2^*) \\ - \frac{j\varepsilon}{8} (\psi_1 - \psi_2 - \psi_1^* + \psi_2^*)^3 = 0, \end{aligned} \quad (68)$$

where \* denotes complex conjugate. These equations are exact.

We now introduce the slow-fast dynamics partition by approximating the complex variables as,

$$\psi_i(t) = \phi_i(t) \exp^{jt}, \quad i = 1, 2, \quad (69)$$

where  $\phi_i(t)$  is assumed to be a slowly varying complex amplitude and the exponential models the fast oscillation with frequency nearly to unity. Substituting this partition into (67), (68) and averaging out components with fast frequencies higher than unity, we obtain the approximate complex modulation equations:

$$\begin{aligned} \dot{\phi}_1 + \left(\frac{j + \varepsilon\lambda}{2}\right) \phi_1 - \frac{3j}{8} (1 - \varepsilon)\phi_1^2 \phi_1^* \\ - \frac{3j\varepsilon}{8} (\phi_1 - \phi_2)^2 (\phi_1^* - \phi_2^*) = 0, \end{aligned} \quad (70)$$

$$\dot{\phi}_2 + \frac{\varepsilon\lambda}{2} \phi_2 + \frac{3j\varepsilon}{8} (\phi_1 - \phi_2)^2 (\phi_1^* - \phi_2^*) = 0. \quad (71)$$

We now introduce the following transformation that accounts approximately for the decay due to damping:

$$\phi_i(t) = \sigma_i(t) \exp^{-\varepsilon t/2}, \quad i = 1, 2 \quad (72)$$

and express the complex amplitudes as:

$$\begin{aligned} \sigma_1(t) = M \sin \theta(t) e^{j\delta_1(t)} \\ \text{and } \sigma_2(t) = M \cos \theta(t) e^{j\delta_2(t)}, \end{aligned} \quad (73)$$

where  $M$  represents a (constant) real amplitude, and where  $\theta(t)$ ,  $\delta_{1,2}(t)$  are angles. Substituting these transformations into Eqs. (70), (71), separating real and imaginary parts and manipulating the resulting differential equations, we obtain the following equations governing the (slow) evolution of the angle  $\theta(t)$  and the phase difference  $\delta(t) = \delta_1(t) - \delta_2(t)$ :

$$\begin{aligned} \dot{\theta} + \frac{3}{8} \varepsilon M^2 e^{-\varepsilon\lambda t} [(\sin \theta - \cos \theta \cos \delta)^2 \\ + \cos^2 \theta \sin^2 \delta] \sin \delta = 0 \end{aligned} \quad (74)$$

$$\begin{aligned} \dot{\delta} + \frac{1}{2} - \frac{3}{8} (1 - \varepsilon) M^2 e^{-\varepsilon\lambda t} \sin^2 \theta \\ - \frac{3}{8} \varepsilon M^2 e^{-\varepsilon\lambda t} [(\sin \theta - \cos \theta \cos \delta)^2 + \cos^2 \theta \sin^2 \delta] \\ \times (\tan \theta - \cot \theta) \cos \delta = 0. \end{aligned} \quad (75)$$

We note that the requirement of slow evolution of the variables  $\theta(t)$  and  $\delta(t)$  poses the restriction that the difference  $\frac{1}{2} - \frac{3}{8}(1 - \varepsilon)M^2 e^{-\varepsilon\lambda t} \sin^2 \theta$  in Eq. (75) be small (actually, it can be shown that this difference must be of  $O(\sqrt{\varepsilon})$ ).

The corresponding approximations for the responses of the system are given by

$$x(t) \sim M \sin \theta e^{-\varepsilon\lambda t/2} \sin[t + \delta(t) + \delta_0], \quad (76)$$

$$y(t) \sim M \cos \theta e^{-\varepsilon\lambda t/2} \sin[t + \delta_0], \quad (77)$$

where  $\delta_0$  depends on the initial conditions of the problem. The approximate Eqs. (74), (75) are defined on a 2-torus and govern (to the first order of approximation) resonance capture in the system under consideration. We note that  $\delta_0 = 0$  and  $\theta(0) = 0$  correspond to zero initial conditions for the original problem except for  $\dot{x}(0) = M$ . Therefore the modulation Eqs. (74), (75) can help us interpret the direct numerical simulations of Figs. 8–10.

For fixed  $M$ ,  $\varepsilon = 0.1$  and  $\lambda = 0.5$ , Eqs. (74), (75) were numerically integrated subject to specific initial conditions  $\theta(0)$  and  $\delta(0)$ . By setting  $\delta_0 = 0$ ,  $\delta(0) = 0$  and  $\theta(0) = 0.1$  (setting the initial condition for  $\theta$  to exactly zero leads to numerical instabilities) we investigate the evolution of the variables  $\theta(t)$  and  $\delta(t)$  for the low- and high-excitation numerical simulations of Figs. 8–10 corresponding to initial excitation of the linear oscillator with initial velocity  $M$  and zero for the other initial conditions. In Fig. 11 we depict the evolution of  $\theta(t)$  and  $\delta(t)$  for  $M = 1.6$  (case of no resonance capture—cf. Fig. 8) and  $M = 3.0$  (case of resonance capture—cf. Fig. 9).

For  $M = 1.6$  no resonance capture occurs;  $\delta(t)$  decreases monotonically with time and  $\theta(t)$  assumes small  $O(\sqrt{\varepsilon})$  values. In this case the motion remains mainly confined to the (initially excited) linear oscillator and only a small portion of the energy is ‘pumped’ to the non-linear oscillator. When we increase the amplitude to  $M = 3.0$ ,  $\delta(t)$  becomes oscillatory for some initial time interval,  $0 < t < 40$ , before assuming a monotonic decrease for  $t > 40$ . The initial oscillatory regime is due to resonance capture in the region of the phase space defined by the neighborhood of the homoclinic loop of the stable periodic solution of the undamped system. After the initial resonance capture, the solution ‘escapes’ the resonance regime and from then on  $\delta(t)$  behaves as in the non-resonance capture

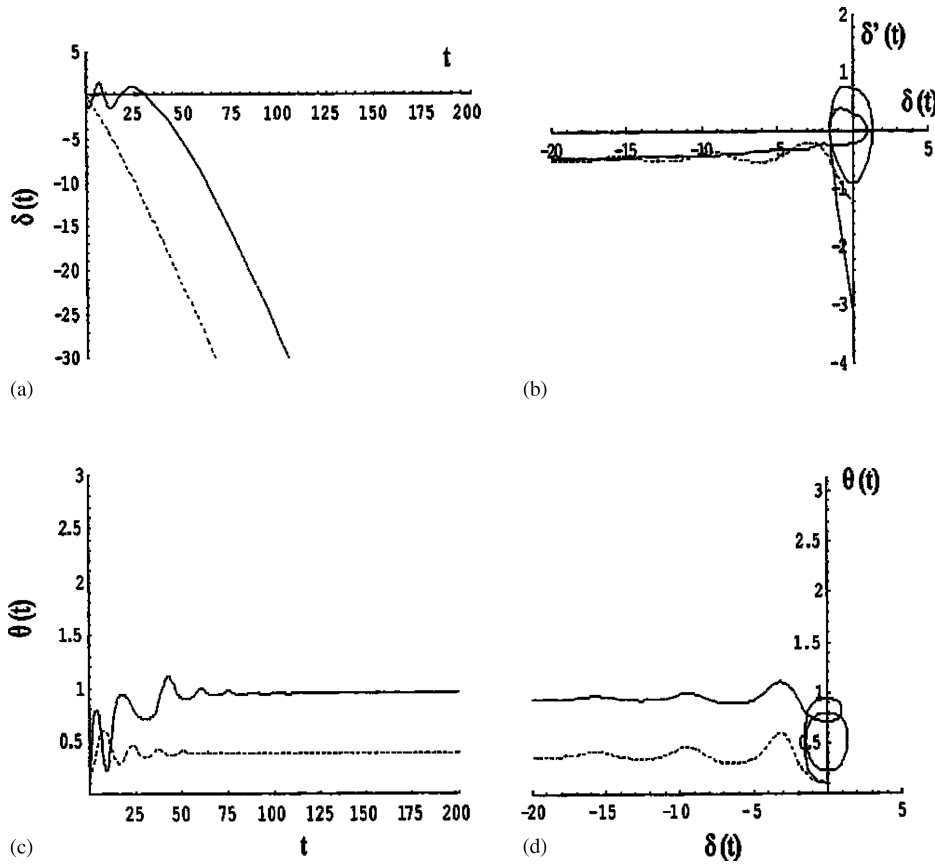


Fig. 11. The evolution of the angles and for  $M = 1.6$  (dashed line), and  $M = 3.0$  (solid line).

case. Considering the behavior of the other angle variable  $\theta(t)$ , it initially increases to  $O(1)$  values during the initial resonance capture regime. In view of Eqs. (76), (77), this implies a one-way energy transfer from the initially excited linear oscillator to the non-linear one. It follows that *resonance capture is associated with oscillatory behavior of  $\delta(t)$  (which leads to the increase of  $\theta(t)$ ), and, thus, to non-linear energy pumping), whereas, absence of resonance capture is associated with monotonic decrease of  $\delta(t)$  (and  $O(\sqrt{\epsilon})$  values of  $\theta(t)$ , i.e., absence of resonance pumping)*. These results establish a direct link between resonance capture and passive non-linear energy pumping in the damped system.

Although the results of this section apply to the specific system (61), (62), they can be extended to all four classes of undamped systems A–D discussed in the

previous sections. It is anticipated that the addition of damping transforms the homoclinic and heteroclinic loops of the undamped slow dynamics into resonance capture regions. Trajectories of the damped system that are temporarily captured in these regimes cause interesting energy exchange phenomena between oscillators, similar to the passive energy pumping exchange described in this section.

### 8. Conclusions

We studied the resonant dynamics of a two-DOF system of non-linear coupled oscillators. One of the oscillators possessed a strong, essential (non-linearizable) cubic non-linearity. For the undamped system this led to a series of internal

resonances, depending on the level of (conserved) total energy of oscillation. We studied in detail the case of 1:1 internal resonance and constructed the bifurcation diagram in parameter space. In the neighborhood of 1:1 resonance the undamped system admits stable and unstable synchronous periodic motions (non-linear normal modes—NNMs). Depending on the system parameters, asynchronous periodic motions (elliptic orbits—EOs) can also be realized.

When damping is introduced, the stable NNMs become damped free oscillations (damped NNMs), and in certain cases produce resonance capture phenomena: a trajectory of the damped dynamics gets ‘captured’ in a neighborhood of a damped NNM before ‘escaping’ and becoming an oscillation with exponentially decaying amplitude. It was shown that such sustained resonance captures produce passive non-linear energy pumping phenomena from the linear to the non-linear oscillator, thus sustained resonance capture appears to provide a dynamical mechanism for passively transferring energy from one part of the system to another, in a one-way, irreversible fashion. The analysis performed in this paper indicates that energy pumping (or equivalently, sustained resonance capture), is affected by the initial conditions of the system, by its initial energy level, and by the specific spatial distribution of the external excitation. We note that energy pumping is directly related to the essential (non-linearizable) stiffness non-linearity of the system [8,7].

As a possible extension of this work we suggest a more general study of the relation between sustained resonance capture and passive energy pumping in a general class of damped oscillators; in this work this relation was studied only for a specific system configuration. In addition, it will be of interest to study energy exchange phenomena related to the excitation of the damped analogs of the stable EOs; in this work we only examined energy transfer related to damped NNMs. In general, this work demonstrates that systems with essential non-linearities possess interesting free and forced dynamics, which can provide

new tools for effective vibration and shock isolation of mechanical systems.

## References

- [1] A.H. Nayfeh, D. Mook, *Nonlinear Oscillations*, Wiley Interscience, New York, 1985.
- [2] R.H. Rand, D. Armbruster, *Perturbation Methods, Bifurcation Theory and Computer Algebra*, Springer, New York, 1987.
- [3] A. Luongo, A. Di Egidio, A. Paolone, On the proper form of the amplitude modulation equations for resonant systems, *Nonlinear Dyn.* 27 (2002) 237–254.
- [4] A. Luongo, A. Paolone, A. Di Egidio, Quantitative analysis of classes of motion for multiresonant systems I. An algebraic method, *Nonlinear Dyn.*, submitted for publication.
- [5] D. Quinn, Resonance capture in a three degree of freedom mechanical system, *Nonlinear Dyn.* 14 (1997) 309–333.
- [6] D. Quinn, Resonant dynamics in strongly nonlinear systems, *Nonlinear Dyn.*, submitted for publication.
- [7] A.F. Vakakis, O. Gendelman, Energy pumping in nonlinear mechanical oscillators: part II—resonance capture, *J. Appl. Mech.* 68 (2001) 42–48.
- [8] A.F. Vakakis, Inducing passive nonlinear energy sinks in linear vibrating systems, *J. Vibr. Acoust.* 123 (2001) 324–332.
- [9] P.G.D. Barkham, A.C. Soudack, An extension of the method of Kryloff and Bogoliuboff, *Int. J. Control* 10 (1969) 377–392.
- [10] P.G.D. Barkham, A.C. Soudack, Approximate solutions of nonlinear nonautonomous second-order differential equations, *Int. J. Control* 11 (1970) 101–114.
- [11] P.G.D. Barkham, A.C. Soudack, New results on the elliptic function method, *Int. J. Control* 26 (1977) 341–358.
- [12] V.T. Coppola, R.H. Rand, Averaging using elliptic functions: approximation of limit cycles, *Acta Mechanica* 81 (1990) 125–142.
- [13] P. Byrd, M. Friedman, *Handbook of Elliptic Integrals for Engineers and Physicists*, Springer, Berlin, 1954.
- [14] B.V. Chirikov, A universal instability of many-dimensional oscillator systems, *Phys. Rep.* 52 (1979) 265–376.
- [15] R.H. Rand, Lecture Notes on Nonlinear Vibrations, <http://www.tam.cornell.edu/randdocs/>, version 45, 2003.
- [16] O. Gendelman, L.I. Manevitch, A.F. Vakakis, R. M’Closkey, Energy pumping in nonlinear mechanical oscillators: part I—dynamics of the underlying Hamiltonian systems, *J. Appl. Mech.* 68 (2001) 34–41.